New Journal of Physics
The open access journal for physics

The effect of phase front deformation on the growth of the filamentation instability in laser–plasma interactions

E Higson[1,2], R Trines[2,8], J Jiang[3], R Bingham[2,4], K L Lancaster[2,6], J R Davies[3,7] and P A Norreys[1,2,5]

[1] University of Oxford, Parks Road, Oxford OX1 3PU, UK
[2] Central Laser Facility, STFC Rutherford Appleton Laboratory, Harwell Oxford, Didcot, Oxfordshire OX11 0QX, UK
[3] GOLP/Instituto de Plasmas e Fusão Nuclear—Laboratorio Associado, Instituto Superior Técnico, 1049-001 Lisbon, Portugal
[4] Physics Department, University of Strathclyde, Glasgow G4 0NG, UK
[5] Blackett Laboratory, Imperial College London, Prince Consort Road, London SW7 2BZ, UK
E-mail: raoul.trines@stfc.ac.uk

New Journal of Physics **15** (2013) 015027 (13pp)
Received 11 September 2012
Published 31 January 2013
Online at http://www.njp.org/
doi:10.1088/1367-2630/15/1/015027

Abstract. Laser pulses of 0.9 kJ/1 ns/1053 nm were focused onto low-Z plastic targets in both spherical and planar geometry. The uniformity of the resulting plasma production was studied using x-ray pinhole imaging. Evidence is provided suggesting that thermal filamentation starts to occur for irradiances on the target of $I\lambda^2 \geqslant 10^{14}\,\mathrm{W\,cm^{-2}}\,\mu\mathrm{m}^2$, even on deployment of phase plates to improve the focal spot spatial uniformity. The experiments are supported by both analytical modelling and two-dimensional particle-in-cell simulations. The implications for the applications of laser–plasma interactions that require high degrees of uniform irradiation are discussed.

[6] Current address: York Plasma Institute, Department of Physics, University of York, Heslington, York YO10 5DD, UK.
[7] Current address: Fusion Science Center, Laboratory for Laser Energetics and Mechanical Engineering, University of Rochester, Rochester, NY 14623, USA.
[8] Author to whom any correspondence should be addressed.

Contents

1. Introduction

There is a wide range of interesting applications for the guiding of intense laser pulses in plasma [1–10]. These include the control over the quality of electrons accelerated in laser wakefield accelerators [11–14], particularly the reproducibility of the electron bunch energy and pointing stability [13–17]. In addition, studies of betatron oscillation x-ray emission from these plasmas require reproducible conditions [18–20].

In shock ignition inertial fusion [21–22], the deuterium–tritium fuel is compressed to high density using a shaped laser pulse designed to assemble the fuel on a low adiabat. About 300 ps before the stagnation point, a strong shock is launched by an additional 'ignitor' laser pulse. This has an irradiance $I\lambda^2 \approx 7 \times 10^{14}$ W cm^{-2} μm^2. The conditions for ignition in the fuel are obtained after collision of the strong shock (driven by the action of the additional laser pulse) with the return shock, which is the outward moving shock associated with the rising pressure in the central hot spot. This scheme combines the advantages of smaller in-flight aspect ratios, leading to reduced hydrodynamic instability growth, with larger fuel mass and thus high fusion energy gain. Most importantly, no additional large-scale changes are needed to existing large-scale facilities, particularly the National Ignition Facility (NIF) and Laser Megajoule (LMJ).

In fast ignition inertial fusion [23], one can choose between several options to deliver the high-intensity ignitor laser pulse securely to the compressed targets. Firstly, the ignitor pulse can be guided to the target core by a cone insert. Good results have been obtained through this method [24], but there are several important drawbacks. The cone material needs to have a large mass density, and high-Z materials are usually employed, but these lead to large energy losses via bremsstrahlung emission and there is the potential for contamination of the fusion fuel with high-Z matter ablated during the compression stage. An alternative method is to use a $\sim$100 ps relativistic intensity laser pulse to drill a channel through the outer layers of tenuous plasma surrounding the compressed core. Once a fairly clean, straight channel has been created this way [25], the ignitor pulse can be launched down this channel, and be guided straight to the compressed core. This removes the need to use high-Z components in the target completely, and also solves the issue of target alignment, as the channel is only drilled after the target has been positioned and the target itself can be spherically symmetric.

The latest experimental studies devoted to channel formation in under-dense plasma have revealed unique and interesting features associated with the use of relatively long pulse duration ($\geqslant$ 10 ps), relativistically intense laser pulses [26–28]. These include clear demonstrations of channel formation at 10^{18} and 6×10^{19} cm^{-3} background electron densities; surface wave formation at the channel walls; unusual (prolate-spheroid) structure of *post-soliton* plasma

cavities formed during the interaction, bifurcation of the channels; and multiple-filamentation of the laser pulse after it has propagated some distance into the plasma.

Filamentation of laser pulses under both high and lower intensity conditions has been studied for many years owing to its importance in all variations of inertial confinement fusion research. The filamentation instability shares many features with stimulated Brillouin scatter [29]. It has the same dispersion relationship, but in this case it occurs in a plane orthogonal to the propagation vector of the laser light wave.

Filamentation can be triggered by various mechanisms [30, 39, 40]. For short pulses at a relativistic intensity ($a_0 > 1$), a relativistic mass increase of the electrons in the laser pulse is the dominant effect. Such a mass increase lowers the (relativistic) plasma frequency and thus the refractive index of the plasma. Laser intensity fluctuations then lead to fluctuations in the refractive index, which feeds back into the laser propagation and triggers filamentation. For longer pulses, there will be a competition between ponderomotive filamentation and thermal filamentation [30]. The ponderomotive force that a laser pulse exerts on the plasma tends to push electrons away from the regions where the laser intensity is highest. This leads to a localized decrease in the plasma frequency and thus the plasma refractive index. Once again, this feeds back into the laser propagation in a way that triggers filamentation. For dense plasma with a high collision rate, the ponderomotive mechanism is less effective. In that case, much of the laser energy will be absorbed by the plasma through collisional effects. This causes localized heating and expansion of the plasma, and thus a decrease in plasma frequency, in those regions where the laser intensity is highest. Filamentation is then triggered in a similar fashion as for ponderomotive filamentation. It has been shown [30] that thermal filamentation will be dominant over ponderomotive filamentation when the electron mean free path length is less than 6% of the filament width.

The laser and plasma conditions investigated in this paper are such that the filamentation is predominantly ponderomotive. In that case, the criteria for significant growth of the thermal filamentation instability can be written as [30]

$$\left(\frac{v_0}{v_{\mathrm{Te}}}\right)^2_{\mathrm{Threshold}} = \frac{8\omega_0^2}{\omega_{\mathrm{pe}}^2}\left(\left[\left(0.065/k_0^2\lambda_{\mathrm{mfp}}^2\right)^2 + \left(\gamma_T/\omega_0\right)^2\right]^{1/2} - 0.065/k_0^2\lambda_{\mathrm{mfp}}^2\right), \tag{1}$$

where $v_0 = c^2 k_0/\omega_0$, c is the speed of light, k_0 is the wave number of the laser field, v_{Te} is the electron thermal velocity, ω_0 and ω_{pe} are the laser and electron plasma frequencies, λ_{mfp} is the electron mean free path and $\gamma_T = \frac{\omega_{\mathrm{pe}}^2}{2\nu_{\mathrm{e}}}\frac{v_{\mathrm{Te}}^2}{c^2}\frac{1}{k_0^2\lambda_{\mathrm{mfp}}^2}$. One can estimate that even for 1 keV plasmas and $\omega_0/\omega_p = 2$, corresponding to the coronal plasma temperature for irradiances of $I\lambda^2 \approx 10^{13}\,\mathrm{W\,cm^{-2}}\,\mu\mathrm{m}^2$, there is a significant probability of thermal filamentation growth for low-Z plasmas. In this paper, however, filamentation and bifurcation of laser pulses are studied for $\omega_0/\omega_p = 10$, and in that case thermal filamentation can be neglected with respect to ponderomotive filamentation.

While most studies of filamentation of laser pulses concentrate on fluctuations in the laser pulse intensity, a detailed analysis of the simulations employed in [26] revealed that ripples in the phase fronts of the propagating laser pulse also play an important role. Fluctuations in (the position of) the phase front can cause different parts of the laser pulse to interfere either constructively or destructively, and can eventually cause the laser pulse to break up into two or more strands. An initial investigation of this effect was carried out in [26] to explain the

bifurcation of a laser pulse in a hole-boring experiment. In this paper, we intend to explore the influence of phase front fluctuations on bifurcation and filamentation in more depth.

Given the recent interest in utilising high-intensity interactions for these applications described above, a renewed study of this topic is required. In section 2, a simple quasi-static analytical model is introduced that explores the role of phase changes induced by density gradients as an intense laser pulse propagates in plasma. The results of this model are compared with two-dimensional (2D) particle-in-cell (PIC) simulations and good agreement is found between them. A number of factors are identified as important: the larger the phase change that is induced as the beam propagates, the faster filamentation occurs; the larger the transverse gradient in phase across the wave front, the faster the beam breaks up; and finally once a phase change is induced, filamentation occurs instantaneously. Most importantly, the study reveals that filamentation does not occur in sufficiently narrow sharp channels that are dominated by self-focusing. In section 3, experiments are described in which the threshold for the thermal filamentation is shown to occur for irradiances on the target of $I\lambda^2 \approx 10^{14}\,\mathrm{W\,cm^{-2}}\,\mu\mathrm{m}^2$. In section 4, applications of these results are discussed with respect to channel formation for fast ignition inertial fusion, as well as for scaling shock-ignition experiments to full scale at NIF and LMJ. The results of the combined study are summarized in section 5.

2. Quasi-static model for filamentation

In this section, a background to the development of the quasi-static model is provided. In this model, a low-intensity laser pulse propagates through a plasma with a prescribed density profile (a channel), obtained from 2D PIC simulations of hole boring by relativistic laser beams. The quasi-static model is then presented and is used to explore the deformation of the phase front of the laser beam caused by the transverse plasma density variations across the channel, and the effects of these phase changes on beam filamentation. The model's predictions are then compared with the results of 2D PIC simulations.

The starting point for this model is the interaction of a 25 ps duration ($a_0 = 1$) relativistic intense laser pulse at the edge of an under-dense plasma using an *f*/3 focusing optic. Previous studies [26] have shown that a channel is formed in the plasma by the following mechanism. During the first eight picoseconds, the laser pulse heats the plasma locally at the focal plane, before defocusing. After this time, a small region (smaller than the focal spot) begins to respond hydrodynamically and expands radially outwards. This provides a gradient in density that starts to self-focus the incident laser pulse. The channel then begins to form and rapidly extend into the plasma, far beyond its Rayleigh range. After a certain distance, the channel splits and the laser pulse divides into a number of channels. This is due to the beam propagating through regions of different plasma densities, associated with the formation of the channel walls.

Three factors in the deformation of wave fronts that may affect beam break-up were proposed and investigated: (i) the size of the phase difference (Δphase), (ii) the gradient or sharpness of the phase difference $\left(\frac{\Delta\text{phase}}{\Delta x}\right)$ and (iii) the distance for which the wave travels with this discrepancy (y).

Through the quasi-static model described below, as well as PIC simulations of low-intensity laser beams propagating through plasma with a prescribed density profile, the relative influence of these three factors on the occurrence and extent of laser beam filamentation has been determined. We know from examples in experiments and OSIRIS simulations that a

combination of the first two factors is required for beam break up—a deformation of a wave front by a phase difference of π (distance $(\frac{1}{2})\lambda$) has no effect when spread gradually across a wave front thousands of wavelengths wide. Equally a sharp phase difference of a small fraction of π will not cause filamentation.

Further evolution of the central beam leads to its own break-up and its energy is equally distributed to the two outer beams, resulting in bifurcation of the channel. The position of the bifurcation point also moves rapidly, and a single channel can be re-established after sufficient time.

In the quasi-static model, a plasma profile is used that was taken from a PIC simulation in [26]. In that simulation, a $1.3 \times 10^{18}\,\mathrm{W\,cm^{-2}}$ laser pulse with a $10\,\mu$m focal spot diameter bored a channel in a $300\,\mu$m plasma slab at 1% of the critical density. The following function was used to reproduce the charge density spatial profile from that simulation:

$$f(x, y) = (3.75 \times 10^{-3} u^{16} - 9.5 \times 10^{-3})\exp(-u^4) + 0.01 + 4.0 \times 10^{-3}(\exp(-64u^2)), \tag{2}$$

where

$$x_1 = \frac{35000x}{2\pi \times 10^6}, \quad y_1 = \frac{3333y}{2\pi \times 10^6}, \quad u = x_1\left(1 + \frac{y_1}{2}\right).$$

When modelling of exponential ramp (mimicking an expanding plasma halo) was required, $f(x,y)$ was multiplied by a ramp factor for y less than the scale length of the ramp (L_{ramp}):

$$\mathrm{ramp} = \exp\left[\frac{8(y - L_{\mathrm{ramp}})}{L_{\mathrm{ramp}}}\right].$$

This profile is shown in figure 1. Frames (a) and (b) show the full, 2D extent of the modelled profile $f(x,y)$. Frame (d) shows a cross-section of the channel profile at $x_1 = 5500$. Frame (c) shows a cross-section taken from a typical PIC simulation of channel formation [26] for comparison.

The quasi-static model follows from a consideration of the phase of the wave, ϕ, which is expressed as the total number of radians through which the wave has travelled. For an electromagnetic wave travelling through plasma with a constant electron density (and hence constant ω_{p}) in the direction of wave propagation, $\phi = 2\pi L/\lambda = kL$. After travelling a distance L into the plasma (and because $k = 2\pi/\lambda = \sqrt{\omega_0^2 - \omega_{\mathrm{p}}^2}/c$), it follows that $\phi = (L\omega_0/c)\sqrt{(1 - \omega_p^2/\omega_0^2)}$. When one then considers the phase differences caused by plasma, $\delta\phi$, one defines the relative phase of the wave at a distance x into the plasma as the phase at which the wave would be if it were travelling through a vacuum for distance x minus its actual phase. Hence,

$$\delta\phi = \frac{L\omega_0}{c}\sqrt{1 - \frac{\omega_{\mathrm{p}}^2}{\omega_0^2}} - \left(\frac{L\omega_0}{c}\right). \tag{3}$$

Also, as ω_{p} varies with the distance travelled in the direction of wave propagation L, one integrates the function with respect to L

$$\delta\phi = \int_0^{L_{\max}} \frac{\omega_0}{c}\left(\sqrt{1 - \frac{\omega_{\mathrm{p}}^2}{\omega_0^2}} - 1\right) \mathrm{d}L. \tag{4}$$

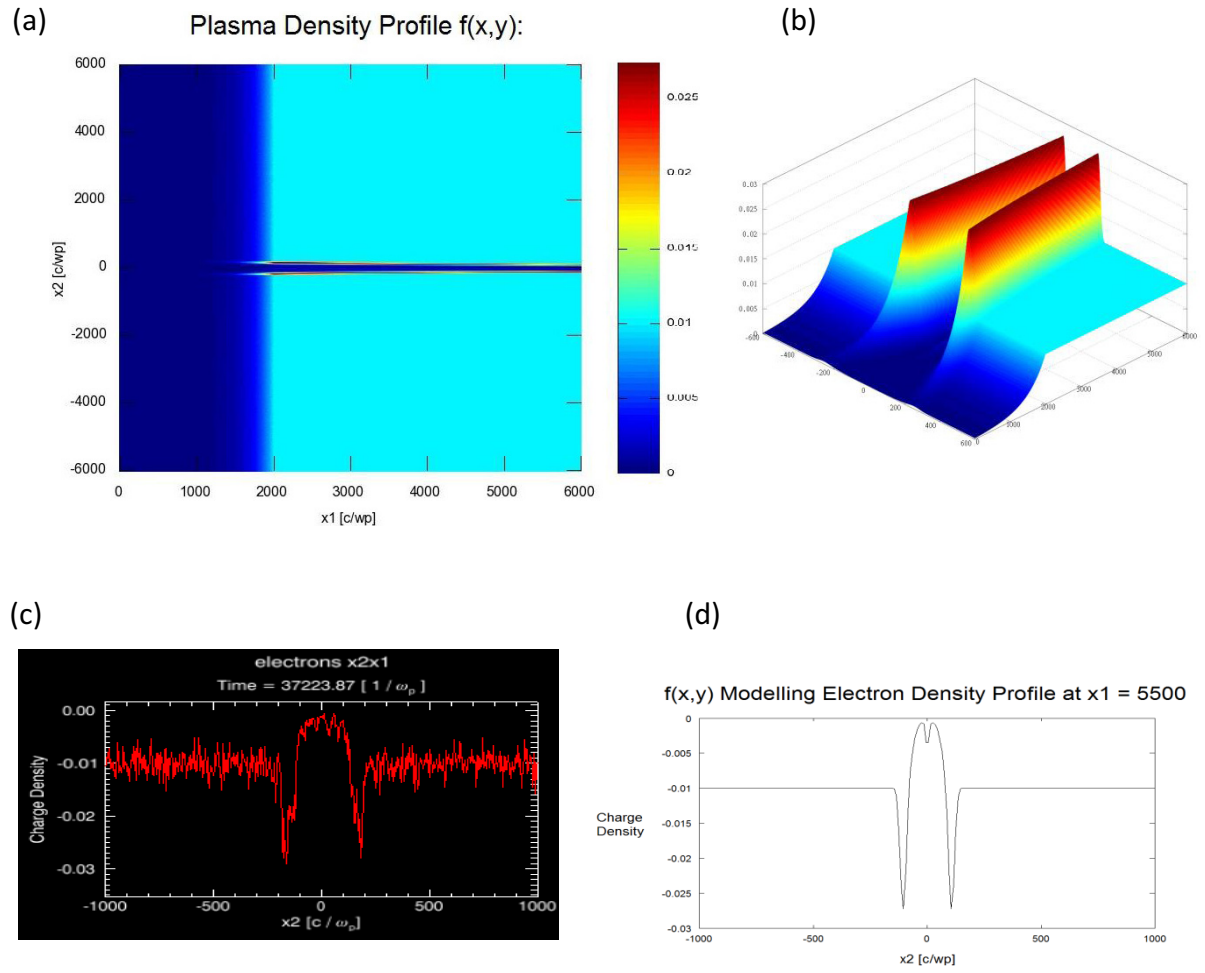

Figure 1. (a), (b) Colour plots of $f(x,y)$ as defined by equation (2), with $L_{\mathrm{ramp}} = 2000$; (c) a line-out through the channel from the PIC simulation of [26] at $x_1 = 5500$; (d) $f(x,y)$ at $x_1 = 5500$, showing good agreement.

One is now able to estimate the phase change that a wave travelling through a 2D slice of plasma experiences by combining (2) and (4)

$$\delta\varphi = \int_0^{Y_{\max}} \frac{\omega_0}{c}\left(\sqrt{1 - f(x,\, y)} - 1\right) \mathrm{d}L, \tag{5}$$

where y is the direction of wave propagation.

In order to verify the predictions of the quasi-static model, a sequence of PIC simulations has been carried out using a reduced laser intensity of $1.3 \times 10^{14}\,\mathrm{W\,cm^{-2}}$, corresponding to $a_0 = 0.01$. This intensity is sufficiently low for the laser pulse not to significantly perturb the plasma, while the effect of the plasma density profile on laser pulse propagation is faithfully preserved. The parameters of these simulations were as follows: the background plasma density was $0.01 n_{\mathrm{cr}}$, laser wave length was 1 μm, spot diameter was 10 μm, plasma channel profile was as given above, the box dimensions were 7825×3016, in units of c/ω_{p}, and the time at which the snapshots were taken was 7519, in units of ω_{p}^{-1}.

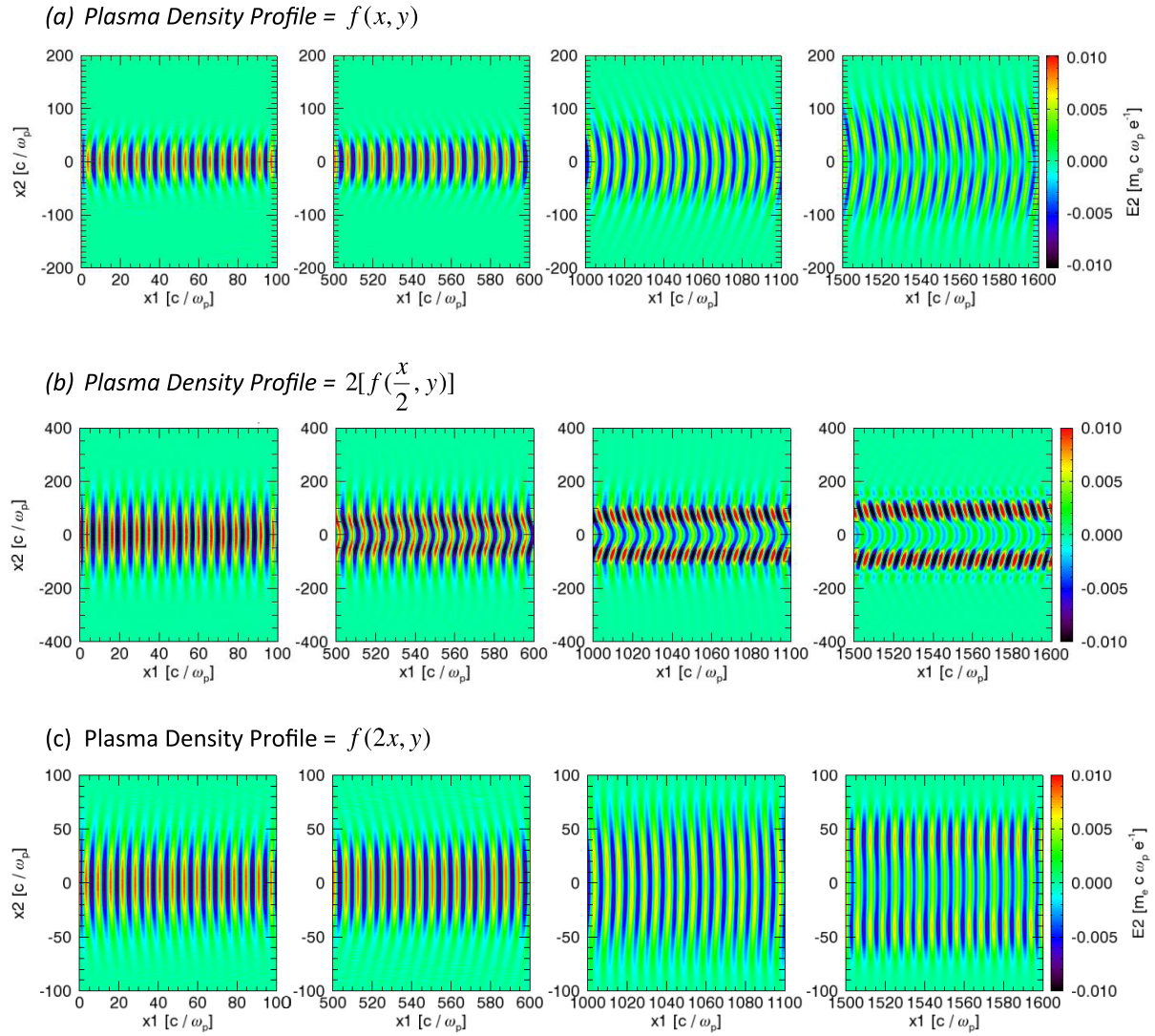

Figure 2. Effects of absolute plasma density and density gradient on laser beam propagation. (a) Propagation in the standard channel given by $f(x,y)$. (b) Propagation in the modified channel $2f(x/2,y)$, so the amplitude of the density perturbation is doubled while the density gradients are preserved. (c) Propagation in the modified channel $f(2x,y)$, so the density gradients are doubled while the amplitude of the density perturbation is preserved.

Figure 2(a) shows the electric field at different times in the simulation, providing information on individual wave fronts, plasma density profiles given by equation (3). Shown in figure 2(b) is its transformation where the plasma density is doubled but its gradient with respect to the transverse direction is kept constant $[2f((\frac{1}{2})x, y)]$. One can clearly see that the greater phase discrepancy between wave fronts, caused by a greater plasma density, causes the beam to bifurcate much faster. This also causes the beamlets to be more focused and intense, as shown by the red colours of the wave fronts.

Figure 2(c) shows a transformation that shrinks the transverse axis by a factor of 2, increasing the transverse spatial gradient of phase change but keeping the other factors constant

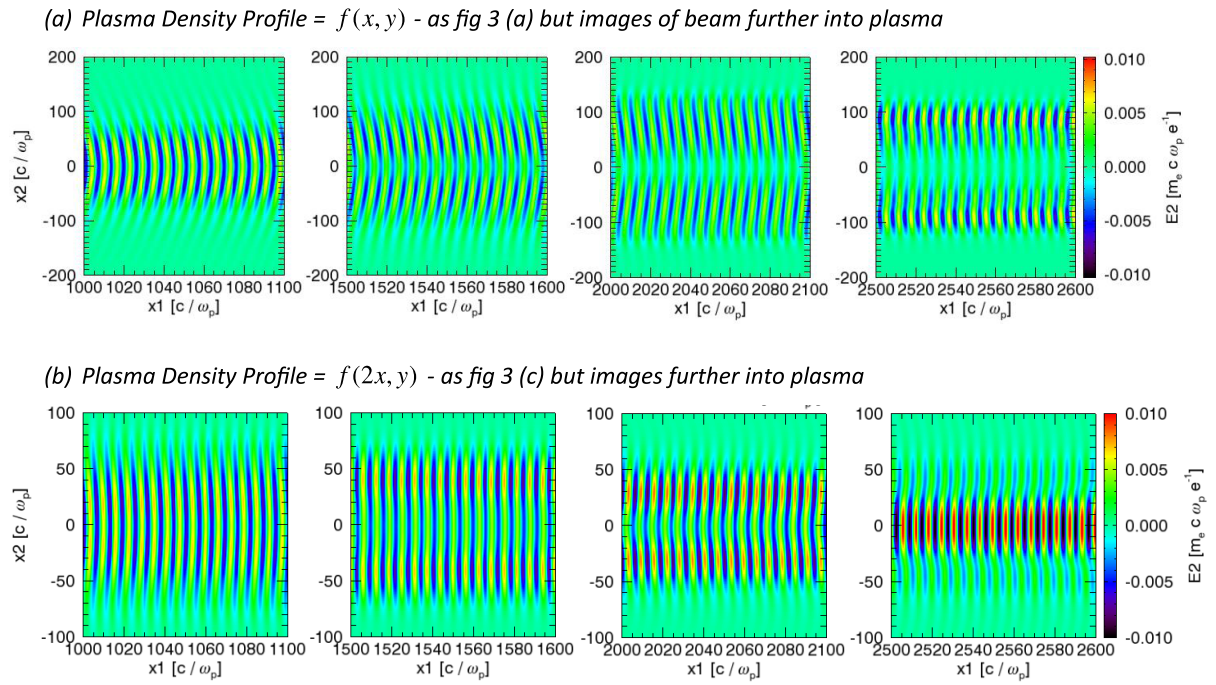

Figure 3. For a very narrow sharp channel, self-focusing effects dominate filamentation and the beam cannot escape the channel.

[$f(2x,y)$]. This requires consideration of the competition between increased self-focusing and the effect of the larger gradient. Comparison of figures 2(a) and (c) provides compelling evidence that the larger gradient does indeed cause the beam to bifurcate faster. If this were not the case, then the increase in self-focusing would mean that the beam would split much more slowly. Hence, this demonstrates that the larger gradient of phase change increases the bifurcation speed.

We also simulated the propagation of the filamented laser beam in vacuum, as a control. As expected, no further filamentation was observed in this case.

Figure 3 shows the same simulations that were used to illustrate effects of a gradient (figures 2(a) and (c)), but this time viewed further into the plasma. The sharp, narrow channel of $f(2x,y)$ creates self-focusing effects so powerful that the bifurcated beam is unable to diverge and is focused back down into a single beam. As discussed in section 1, filamentation can be very unhelpful for most applications and this observation shows that under certain conditions, i.e. with a sufficiently narrow, steep sided channel, the beam will be unable to escape; this has important implications that will be discussed in section 4.

3. Experiments and results

The experiments were conducted on the Nd:glass laser Vulcan [32] in both six-beam cubic and four-beam planar geometry, illustrated in figures 4(a) and 5(a). In the first case, the laser was arranged in six-beam cubic symmetry using *f*/2.5 lenses, but without phase plates. The laser beams overlapped hollow plastic shell targets of 486 μm diameter and 8 μm wall thickness, coupled with a hollow gold-cone insert. This experiment was designed to study the compression

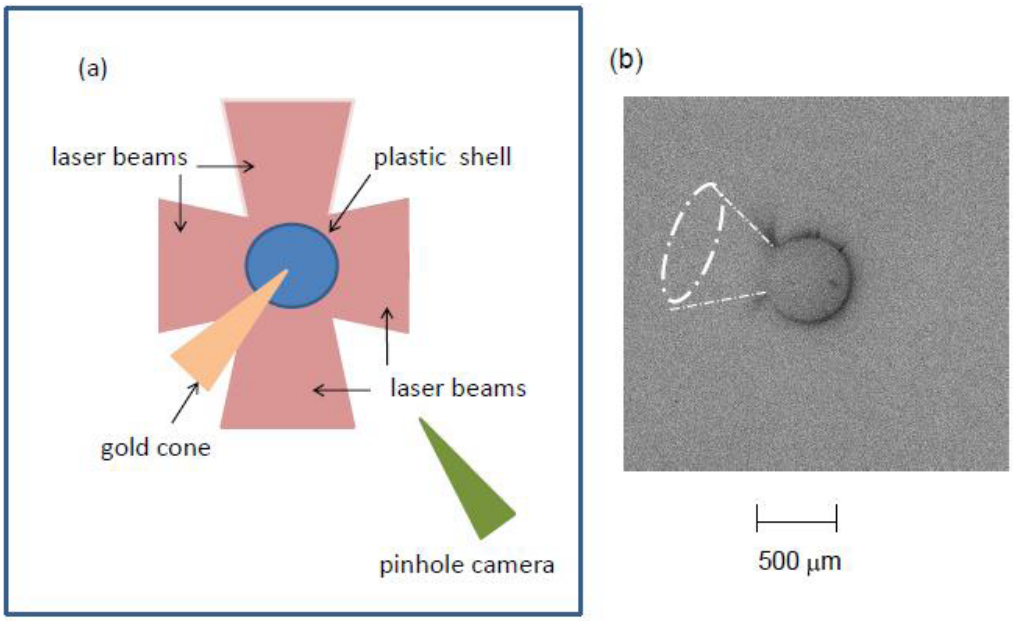

Figure 4. (a) Schematic illustration of the laser beam and diagnostic arrangement and (b) x-ray image of cone–shell irradiated target providing evidence of thermal filamentation.

and fast electron energy coupling in cone-guided fast ignition [33]. The results of that study are reported elsewhere [34]. The laser delivered 1.0 kJ of 1053 nm laser radiation in 1 ns pulse duration to the target, providing an intensity on the target of $I\lambda^2 \approx 1.3 \times 10^{14}\,\mathrm{W\,cm^{-2}}\,\mu\mathrm{m}^2$. The pinhole camera had a 10 μm diameter pinhole which was located 8 cm from the target and had a magnification of $\times 5$. The x-ray images were recorded in a Kodak DEF film. A 25 μm-thick beryllium film filtered the x-rays such that only those photons with energies above 1.0 keV were transmitted. Figure 4(b) illustrates that filamentation can occur under these conditions, but was observed to occur in only 10% of the dataset obtained.

In the second case, the laser was focused onto planar plastic targets with four laser beams using *f*/10 lenses, as illustrated schematically in figure 4(a). This experiment was designed to study channel formation in under-dense plasma for fast ignition [25]. The results of that study are also reported elsewhere [28]. Each beam was equipped with a phase plate to improve the overall irradiation uniformity. The focal spot was 780 μm diameter, providing an irradiance on the target of $I\lambda^2 \approx 1.7 \times 10^{14}\,\mathrm{W\,cm^{-2}}\,\mu\mathrm{m}^2$. In this case, two x-ray pinhole cameras were used. The first one looked directly above the target and the pinhole (comprising a 10 μm-diameter pinhole in a platinum substrate) was located 10 cm from the plasma with a magnification of $\times 4$. The second one also had a 10 μm-diameter pinhole, but was positioned to view the plasma at 60° from the target normal. It was located 7.5 cm away, providing a magnification of $\times 5.6$. In both instruments, Fuji BAS-TR image plates were used to record the x-ray images and were filtered with 25 μm-thick beryllium to record x-ray above 1.0 keV. Evidence for thermal filamentation is shown in figures 5(b) and (c).

It is clear from these observations that, as expected, the threshold for significant growth of the thermal filamentation instability lies in the region $I\lambda^2 \approx 10^{14}\,\mathrm{W\,cm^{-2}}\,\mu\mathrm{m}^2$.

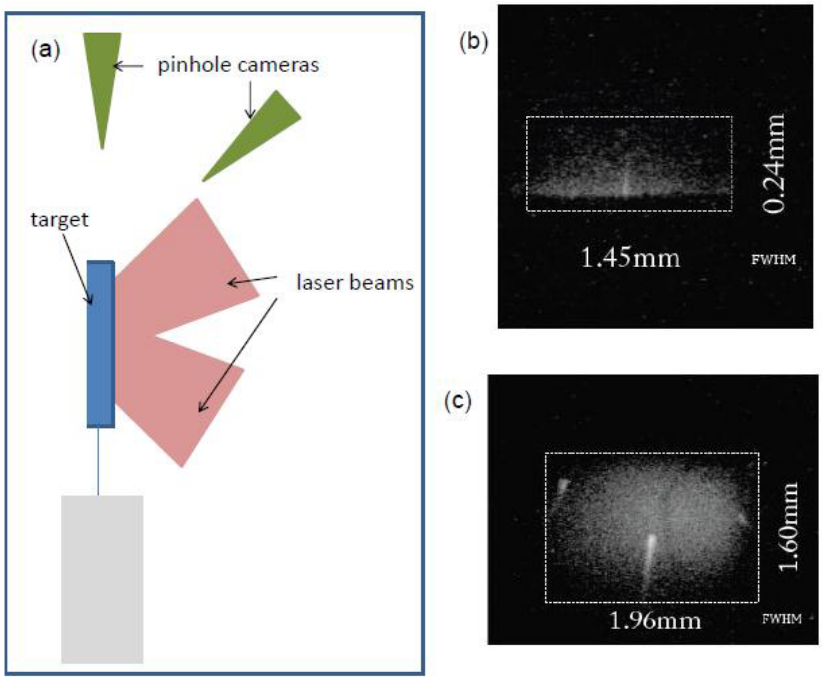

Figure 5. (a) Schematic illustration of the laser beam and diagnostic arrangement, (b) x-ray image of the planar plastic target viewed from the top of the target mount and (c) x-ray image of the planar plastic target viewed from 60° to the target normal.

4. Discussion

In this section, the limitations of the experiments and the quasi-static model are discussed before exploring the implications of channel formation for fast ignition and wakefield accelerator studies. The applications of the scaling of the shock ignition scheme to NIF and LMJ are then described.

The first assumption of the quasi-static model is that the plasma is considered static with time. This is not a problem as the speed of light in plasma is close to its vacuum velocity, and hence over the distance and time scales considered, the plasma density cannot change significantly. The second assumption is that self-focusing effects are neglected in the model. However, this is not a problem as these are included automatically in the OSIRIS simulations. This allows one to infer the essential physics by comparing both the models. The third assumption is that laser pulse propagation in channels formed by relativistic intense laser pulses behaves in a similar fashion to lower intensity cases. This limitation of the model means that it can only be used to study propagation in preformed channels where the refractive index gradients are determined by the background plasma profile itself, rather than the increase in rest mass of electrons expelled as a result of the ponderomotive force.

Having said that, it is worth reiterating the knowledge gained from the model and the comparisons with OSIRIS simulations. These are: larger changes in $\delta\phi$ implies faster beam breakup; gradient $(\mathrm{d}\phi/\mathrm{d}x)$ implies faster beam break-up; beak-up effects caused by $\delta\phi$ happen almost instantaneously; and filamentation does not occur in sufficiently narrow sharp channels.

These results imply that the use of a faster focusing optic, or the use of shorter wavelength pulses with similar a_0 and f-number, will prevent bifurcation and channel splitting. This could have implications for laser wake-field accelerator studies where long propagation distances in plasma are required. In this case, the channel formation pulse would be followed by an ultra-short pulse to excite the blow-out/bubble regime. The results also suggest that there is an option for guiding the heating pulse for fast ignition inertial fusion, when integrated target designs require reduced channel formation pulse duration. Certainly, the results are consistent with electron acceleration experiments using dual-collinear laser pulses [17].

An experimental study, reported in the early 1980s from Moscow's Lebedev Institute, revealed that extensive filamentation in coronal plasma did occur for low-Z plastic targets, in agreement with those expected from equation (1). In their case, spherical plastic shell targets were irradiated using the 1 kJ/1 ns/1053 nm DELFIN laser facility with irradiances on the target of $I\lambda^2 \approx 5 \times 10^{13}\,\mathrm{W\,cm^{-2}}\,\mu\mathrm{m}^2$ [35]. Of course, those experiments were conducted before the invention of phase plates in 1985 which provide a more uniform spatially irradiation pattern in the focal plane [36], and smoothing by spectral dispersion (SSD) [37]. The experiments described in section 3 have shown that the threshold for the filamentation instability is, as expected, in the range $I\lambda^2 \approx 10^{14}\,\mathrm{W\,cm^{-2}}\,\mu\mathrm{m}^2$ (three times higher than the earlier Lebedev results). Because the filamentation instability is convective in nature, the filamentary structure amplifies as it propagates through the plasma, making it a dangerous instability in long-scale length plasmas. It is also less affected by density gradients than the normal three-wave instabilities, and therefore adding additional temporal smoothing techniques, such as 2D SSD, despite reducing the growth rate slightly, cannot control it entirely.

Of course, preliminary experimental studies of shock ignition have been conducted at the OMEGA laser facility at the University of Rochester and have generated some encouraging and positive results [22]. In particular, cryogenic deuterium–tritium shells generated areal densities close to one-dimensional predictions and about 12% of the predicted fusion yield. It is interesting to note that the adiabatic compression was accomplished by uniformly irradiating the target with 40 of the 60 beams, while the final shock was formed by focusing the remaining laser beams onto the critical surface with much smaller focal spots, in this case 50 μm diameter. As a result, no filamentation of the target was observed in x-ray imaging. One can understand this in light of the reduced growth of the filamentation instability in restricted channels described in section 2, figure 3.

However, when one scales the shock ignition scheme from OMEGA to LMJ or to NIF, then one finds that the critical density surface is located 400–500 μm from the target centre when the shock ignition pulse is first introduced. Near spherical illumination is needed to deliver the intensity required for driving the shock from there. This risks growth of the filamentation instability, particularly given that the intensity requirement is well above the threshold confirmed here in this paper. Therefore, it is recommended that the shock ignition pulses are focused into tight beams in the coronal plasma, possibly at the edge of the original target surface (similar to the OMEGA laser case), to avoid filamentation growth in the coronal plasma. Only future experiments can determine whether the filamentation instability becomes a significant issue in the long-scale-length plasmas expected under these conditions.

Finally, one must state that the computer simulations are restricted to 2D, whereas three-dimensional effects, such as braiding of intense laser filaments [38], are left for a future study.

5. Summary

In this paper, a quasi-static model for phase front deformation on beam filamentation has been presented. By comparing the model with 2D PIC simulations, the following processes have been identified as important: larger changes in $\delta\phi$ with the propagation distance implies a faster beam break-up; larger transverse gradients ($\mathrm{d}\phi/\mathrm{d}x$) implies a faster beam break up; break-up effects caused by $\delta\phi$ happen almost instantaneously; and filamentation can be prevented in sufficiently narrow, sharp-edged channels. Experiments have been described in which the growth of the filamentation instability is shown to be in the region of $I\lambda^2 \approx 10^{14}\,\mathrm{W\,cm^{-2}}\,\mu\mathrm{m}^2$, even on deployment of phase plates to improve the focal spot uniformity. The model has been used to identify a number of scenarios where the deleterious nature of the instability can be controlled.

Acknowledgments

The authors thank all the staff of the Central Laser Facility, STFC Rutherford Appleton Laboratory for their assistance with this work. The computer simulations were performed on the SCARF-LEXICON II facility, operated by STFC's e-Science department. The authors also thank the IST/UCLA collaboration for the use of the OSIRIS code. The study was performed under the HiPER preparatory project.

References

[1] Max C, Arons J and Langdon A B 1974 *Phys. Rev. Lett.* **33** 209
[2] Sprangle P, Tang C-M and Esarey E 1987 *IEEE Trans. Plasma Sci.* **15** 145
[3] Durfee C G III and Milchberg H M 1993 *Phys. Rev. Lett.* **71** 2409
[4] Young P E, Hammer J H, Wilks S C and Kruer W L 1995 *Phys. Plasmas* **2** 2825
[5] Young P E, Foord M E, Hammer J H, Kruer W L, Tabak M and Wilks S C 1995 *Phys. Rev. Lett.* **75** 1082
[6] Krushelnick K, Ting A, Moore C I, Burris H R, Esarey E, Sprangle P and Baine M 1997 *Phys. Rev. Lett.* **78** 4047
[7] Borghesi M, MacKinnon A J, Barringer L, Gaillard R, Gizzi L A, Meyer C, Willi O, Pukhov A and Meyer-ter-Vehn J 1997 *Phys. Rev. Lett.* **78** 879
[8] Fuchs J, Malka G, Adam J C, Amiranoff F, Baton S D, Blanchot N, Héron A, Laval G, Miquel J L, Mora P, Pépin H and Rousseaux C 1998 *Phys. Rev. Lett.* **80** 1658
[9] Tanaka K A, Hashimoto H, Kodama R, Mima K, Sentoku Y and Takahashi K 1999 *Phys. Rev.* E **60** 3283
[10] Najmudin Z, Krushelnick K, Tatarakis M, Clark E L, Danson C N, Malka V, Neely D, Santala M I K and Dangor A E 2003 *Phys. Plasmas* **10** 438
[11] Tajima T and Dawson J M 1979 *Phys. Rev. Lett.* **43** 267
[12] Mangles S P D *et al* 2004 *Nature* **431** 535
[13] Geddes C G R *et al* 2004 *Nature* **431** 538
[14] Faure J *et al* 2004 *Nature* **431** 541
[15] Leemans W P, Nagler B, Gonsalves A J, Tóth C S, Nakamura K, Geddes C G R, Esarey E, Schroeder C B and Hooker S M 2006 *Nature Phys.* **2** 696
[16] Rowlands-Rees T P *et al* 2008 *Phys. Rev. Lett.* **100** 105005
[17] Thomas A G R *et al* 2008 *Phys. Rev. Lett.* **100** 255002
[18] Malka V, Faure J, Gauduel Y A, Lefebvre E, Rousse A and Ta Phouc K 2008 *Nature Phys.* **4** 447
[19] Faure J, Rechatin C, Norlin A, Lifschitz A, Glinec Y and Malka V 2006 *Nature* **444** 737

[20] Kneip S *et al* 2008 *Phys. Rev. Lett.* **100** 105006
[21] Betti R, Zhou C D, Anderson K S, Perkins L J, Theobald W and Solodov A A 2007 *Phys. Rev. Lett.* **98** 155001
[22] Theobald W *et al* 2008 *Phys. Plasmas* **15** 056306
[23] Tabak M, Hammer J, Glinsky M E, Kruer W L, Wilks S C, Woodworth J, Campbell E M, Perry M D and Mason R J 1994 *Phys. Plasmas* **1** 1626
[24] Kodama R *et al* 2001 *Nature* **412** 798
[25] Li G, Yan R, Ren C, Wang T-L, Tonge J and Mori W B 2008 *Phys. Rev. Lett.* **100** 125002
[26] Sarri G *et al* 2010 *Phys. Plasmas* **17** 113303
[27] Willingale L *et al* 2011 *Phys. Rev. Lett.* **106** 105002
[28] Sarri G *et al* 2010 *Phys. Rev. Lett.* **105** 175007
[29] Kruer W L 2003 *The Physics of Laser–Plasma Interactions* (Oxford: Westview Press)
[30] Bingham R, Short R, Williams E, Villeneuve D and Richardson M C 1984 *Plasma Phys. Controlled Fusion* **26** 1077
[31] Fonseca R A *et al* 2002 OSIRIS: a three-dimensional, fully relativistic particle in cell code for modeling plasma based accelerators *Computational Science—ICCS 2002* (*Lecture Notes in Computer Science* vol 2331) p 342
[32] Danson C N *et al* 1998 *J. Mod. Opt.* **45** 1653
[33] Norreys P A *et al* 2004 *Phys. Plasmas* **11** 2746
[34] Key M H *et al* 2008 *Phys. Plasmas* **15** 022701
[35] Aleksandrova I V, Basov N G, Galichii A A, Danilov A E, Kalashnikov M P, Yu. Mikhailov A, Rode A V, Sklizkov G V and Fedotov S I 1983 *JETP Lett.* **38** 68
[36] Kato Y, Mima K, Miyanaga N, Arinaga S, Kitagawa Y, Nakatsuka M and Yamanaka C 1984 *Phys. Rev. Lett.* **53** 1057
[37] Rothenberg J E 1997 *J. Opt. Soc. Am.* B **14** 1664
[38] Ren C, Hemker R G, Fonseca R A, Duda B J and Mori W B 2000 *Phys. Rev. Lett.* **85** 2124
[39] Kaw P K, Schmidt G and Wilcox T 1973 *Phys. Fluids* **16** 1522
[40] Max C E, Arons J and Langdon A B 1974 *Phys. Rev. Lett.* **33** 209